JOURNAL OF GUIDANCE, CONTROL, AND DYNAMICS
Vol. 31, No. 5, September–October 2008

Dynamics and Control of Gravity Tractor Spacecraft for Asteroid Deflection

Bong Wie*
Iowa State University, Ames, Iowa 50011-2271

DOI: 10.2514/1.32735

Multiple gravity tractors in halo orbits and a hovering solar sail gravity tractor are proposed as an option for deflecting a certain class of near-Earth asteroids that may not require high-energy deflection techniques employing nuclear explosions or kinetic impactors. This paper presents the preliminary dynamic modeling and control analysis of such variants of the gravity tractor for examining their practical viability as applied to asteroid Apophis; however, detailed system-level tradeoffs are not treated in this paper. A system of orbiting multiple gravity tractors has many advantages over the hovering gravity tractor. They include its larger total ΔV capability, multispacecraft redundancy, and mission design flexibility with smaller satellites equipped with lower-risk propulsion systems. A solar sail gravity tractor concept exploits the propellantless nature of solar reflectors despite its inherent drawback of requiring a particular hovering position with a 55-deg offset angle from the target asteroid's flight direction.

I. Introduction

THE technically challenging astrodynamic control problem of deflecting near-Earth objects (NEOs) to mitigate their probable impacts upon the Earth is described in this section. A brief historical overview as well as key technical issues of such a complex NEO deflection problem are also described. This section is intended to provide the readers with a self-contained but concise description of the NEO deflection problem of practical significance.

The spectacular collision of comet Shoemaker-Levy 9 with Jupiter in July 1994 was clear evidence of the fact that the risk of impacts upon the Earth by NEOs is very real. In response, the U.S. Congress funded a 10-year survey to locate and track 90% of the NEOs with diameters of 1 km or greater, the impacts of which could threaten the extinction of civilization. In the course of this search, hundreds of thousands of smaller asteroids have been discovered, many similar in size to the 60-m object that exploded above Tunguska, Siberia, on 30 June 1908 with an estimated energy level of 10 Mton of TNT, destroying essentially everything within a 25-km radius. Air bursts with an energy level of 5 kton of TNT, such as that due to the 10-m object that disintegrated over Tagish Lake, Canada, in 2000, are estimated to occur on an annual basis [1].

It is now widely accepted by scientists that an impact by a large asteroid of greater than 10 km in diameter caused the extinction of the dinosaurs 65 million years ago. A 2-km object is known to be capable of causing catastrophic alteration of the global ecosystem, which may lead to the end of civilization. Ocean impacts of even smaller objects are of some concern because the destructive potential caused by the resulting tsunamis may be above that from a same-sized object's land impact. The probability of a major impact to cause the extinction of humanity is extremely low, but it is not zero. Unlike many other natural disasters, such as earthquakes, tsunamis, hurricanes, and tornadoes, which cannot be prevented, the impact threat posed by NEOs can be mitigated given adequate warning time. The impact of an object smaller than 50 m in diameter is often naturally mitigated by the Earth's atmosphere. As the typical small meteoroids enter the atmosphere, they often burn up or explode before they hit the ground. If they burn up, they are called meteors; if they explode, they are called bolides.

A near-Earth asteroid (NEA) refers to any asteroid with a perihelion of less than 1.3 AU. If comets are included, then we speak of NEOs. If a NEA's perihelion is less than that of Earth and its aphelion is greater than that of Earth, it is referred to as an Earth-crossing asteroid. All asteroids with an Earth minimum orbit intersection distance of 0.05 AU or less and an absolute magnitude of 22.0 or less are considered to be potentially hazardous asteroids. Asteroids that cannot get any closer to the Earth than 0.05 AU ($\approx 117 R_{\oplus}$) or are smaller than about 150 m in diameter are not considered potentially hazardous asteroids. A comet sometimes experiences net thrust caused by evaporating ices; this thrust varies significantly as a function of radial distance from the sun, the comet's rotational axis and period, and the distribution of ices within the comet's structure. The precise trajectories of comets are thus less predictable, and an accurate intercept is correspondingly more complex. Fortunately, the threat posed by comets appears to be small compared with the risks of impacts by NEAs, and thus NEO researchers currently focus on mitigating the threat posed mostly by NEAs. However, a further study should continue to address the difficult task of detecting and deflecting comets.

Early detection, accurate tracking, reliable precision orbit calculation, and characterization of physical properties of NEAs are prerequisites to any space mission of deflecting NEAs. The early discovery of NEAs before impact using current ground-based optical sensors is not assured, and detection/tracking of small (1 km or less) NEAs is a difficult task given their low albedo and small size. Various concepts and approaches for advanced ground-based as well as space-based detection systems are being developed to allow for adequate warning time [2].

Assuming that NEAs on a collision course can be detected before impact with a mission lead time of at least 10 years, however, the challenge becomes eliminating their threat, either by destroying the asteroid or by altering its trajectory so that it will miss Earth. A variety of schemes, including a nuclear standoff detonation, mass drivers, kinetic-energy projectiles, laser beaming, and low-thrust deflection via electric propulsion or solar sails, have been already extensively investigated in the past for such a technically challenging asteroid deflection problem [3–7]. The feasibility of each approach to deflect an incoming hazardous object depends on its size, spin rate, composition, the mission lead time, and many other factors. Nuclear standoff explosions are often assessed to be much more effective than the nonnuclear alternatives, especially for larger asteroids with a short mission lead time. Other techniques involving the surface or subsurface use of nuclear explosives are also assessed to be more efficient, although they may run an increased risk of fracturing the

Received 10 June 2007; revision received 4 April 2008; accepted for publication 11 April 2008.

*Vance Coffman Endowed Chair Professor, Department of Aerospace Engineering, 2271 Howe Hall, Room 2355; bongwie@iastate.edu. Associate Fellow AIAA.

target asteroid. The Near-Earth Asteroid Rendezvous (NEAR) mission study of asteroid Mathilde and the Japanese Hayabusa mission for exploring the near-Earth asteroid Itokawa suggest that many asteroids are essentially rubble piles. Computer simulations show that a thermonuclear detonation within or near a body of rubble piles would not effectively disperse the constituent fragments, which would continue following the same trajectory toward Earth [8].

Many of the previously proposed low-energy deflection schemes appear to be impractical. These include attaching large solar sails, mass drivers, or high-efficiency electric propulsion systems to a tumbling or spinning asteroid; painting an asteroid to change its albedo to use the Yarkovsky effect; and laser beaming to ablate small amounts of material from the surface of a tumbling asteroid. Some of these schemes may also require an extremely large number of a heavy launch vehicle.

However, a technology does currently exist for an impulsive velocity change caused by the targeted kinetic impact of a spacecraft on the target asteroid's surface. If applied correctly without causing fragmentation of a large asteroid into smaller pieces and if applied long enough before a projected Earth impact, the effect of such an impulsive ΔV would magnify over decades (or even centuries), eliminating the risk of collision with Earth [9–12]. To be most effective, the impacting spacecraft would either have to be massive or moving very fast relative to the asteroid. Because current launch technology limits the mass (including propellant) that can be lifted into an interplanetary trajectory, we are therefore led to consider designs that would maximize impact velocity and that would not require large amounts of fuel. A solar sailing mission concept described in [13–16] uses a 160-m solar sail to deliver a kinetic-energy impactor (150 kg) into a heliocentric retrograde orbit, which will result in a head-on collision with a target asteroid at its perihelion, thus increasing its impact velocity to at least 70 km/s. However, a practical concern of any kinetic impact approach for mitigating the threat of NEAs is the risk that the kinetic impact could result in the fragmentation of NEAs, which could substantially increase the damage upon Earth impact.

Consequently, Lu and Love [17] recently proposed a low-energy asteroid deflection concept using the mutual gravitational force between a hovering spacecraft and a target asteroid as a towline. Although a large 20-ton gravity tractor (GT) spacecraft propelled by a nuclear-electric propulsion system is considered in [17], a smaller 1000-kg GT spacecraft is capable of towing a certain class of near-Earth asteroids such as asteroid 99942 Apophis [18]. It is interesting to notice that such a gravitational coupling/towing concept has been previously proposed for somewhat science-fictional astronomical problems by Shkadov [19] in 1987 and also by McInnes [20] in 2002. Using the same physical principle of gravitationally anchoring the spacecraft to the asteroid, without physical contact between the spacecraft and the asteroid, we may employ solar sails rather than nuclear- or solar-electric propulsion systems to produce the required continuous low-thrust force. Such a solar sail gravity tractor, described in [21], exploits the propellantless nature of solar sails/reflectors for towing asteroids, despite its inherent drawback of requiring an offset hovering position of 55 deg from an asteroid's flight direction.

Because a GT spacecraft hovering in a static equilibrium standoff position requires canted thrusters to avoid plume impingement on the NEA surface [17,18], McInnes [22] recently investigated a GT spacecraft flying in a displaced non-Keplerian orbit (also often called a halo orbit) for a possible fuel-efficient way of towing asteroids. Such a GT spacecraft (not requiring canted thrusters) in a displaced orbit, in fact, has a fuel-efficient advantage over a single hovering GT spacecraft requiring two canted thrusters. However, a GT in a displaced orbit will require a much heavier spacecraft (about 2.8 times heavier than a single hovering GT) if its orbital displacement is the same as the standoff distance of a hovering GT, or it will need to be placed much closer to the target asteroid (at about 59% of the standoff distance of a hovering GT) if its mass is the same as the mass of a hovering GT. Despite such drawbacks, a practical significance of a displaced orbit is that it simply allows many gravity tractors near a target asteroid, resulting in a larger total ΔV capability, multispacecraft redundancy, and mission design flexibility with smaller satellites equipped with lower-risk propulsion systems. Consequently, in this paper, a system of multiple gravity tractors (MGTs) flying in halo orbits near a target asteroid is proposed as a viable near-term option for deflecting a certain class of NEAs such as asteroid 99942 Apophis or other highly porous rubble-pile asteroids.

This paper will present the preliminary dynamic modeling and control analysis of various gravity tractor spacecraft to examine their practical viability as applied to asteroid Apophis. Detailed system-level tradeoffs are not treated in this paper, however. The fundamentals of asteroid deflection dynamics will be discussed in the Appendix. Most recent assessments of the state-of-the-art technologies for deflecting NEAs can be found in [23].

II. Asteroid 99942 Apophis

In this section, the basic orbital characteristics of asteroid 99942 Apophis are briefly described. Throughout the paper, we will use Apophis as an example target asteroid to illustrate the proposed low-energy deflection schemes.

Asteroid 99942 Apophis, previously known by its provisional designation 2004 MN4, was discovered on 19 June 2004. It is a 320-m NEA that is currently predicted to swing by the Earth in 2029 with a probability of 1 in 45,000 for a keyhole passage in 2029 to result in a resonant return to impact the Earth in 2036. Apophis is an Aten-class asteroid with an orbital semimajor axis less than 1 AU, and its mass is estimated to be 4.6×10^{10} kg. It has an orbital period of 323 days about the sun. After its close flyby of the Earth in 2029, it will become an Apollo-class asteroid. It was previously predicted that Apophis will pass about 36,350 km from the Earth's surface on 13 April 2029, slightly higher than the 35,786-km altitude of geosynchronous satellites. Recent observations using Doppler radar at the giant Arecibo radio telescope in Puerto Rico have further confirmed that Apophis will, in fact, swing by at around 32,000 km from the Earth's surface in 2029, but with a very slim chance of resonant return in 2036.

In Table 1, the six classical orbital elements of Apophis in the J2000 heliocentric ecliptic reference frame are provided for epoch = JD 2454200.5 TDB (10 April 2007). Its other orbital properties are perihelion $r_p = 0.746$ AU, aphelion $r_a = 1.0986$ AU, perihelion speed $v_p = 37.6$ km/s, aphelion speed $v_a = 25.5$ km/s, the mean orbital rate $n = 2.2515 \times 10^{-7}$ rad/s, and the mean orbital speed = 30.73 km/s. Further accurate observations of its orbit are expected when it makes fairly close flybys at 0.1 AU from Earth in 2013 and 2021. An extremely small amount of impact ΔV (approximately 0.04 mm/s) in 2026 is required to move Apophis out of a 600-m keyhole area by approximately 10 km in 2029, in case it is going to pass through a keyhole, to completely eliminate any possibility of its resonant return impact with the Earth in 2036 [16,18,24]. Keyholes are very small regions of the first encounter b-plane such that if an asteroid passes through them, it will have a resonant return impact with the Earth [25–28]. Throughout this paper, asteroid 99942 Apophis will be used as an example of target NEAs to illustrate the proposed concepts.

III. Hovering Gravity Tractor with Canted Thrusters

The gravity tractor concept by Lu and Love [17] uses the mutual gravitational force between a hovering spacecraft and a target asteroid as a towline, as illustrated in Fig. 1. Although a 20-ton

Table 1 Orbital elements of asteroid Apophis

Orbital elements	Value
Semimajor axis a, AU	0.9222614
Eccentricity e	0.191059
Inclination i, deg	3.3310
Perihelion argument ω, deg	126.365
Right ascension longitude Ω, deg	204.462
Eccentric anomaly M at epoch, deg	222.273

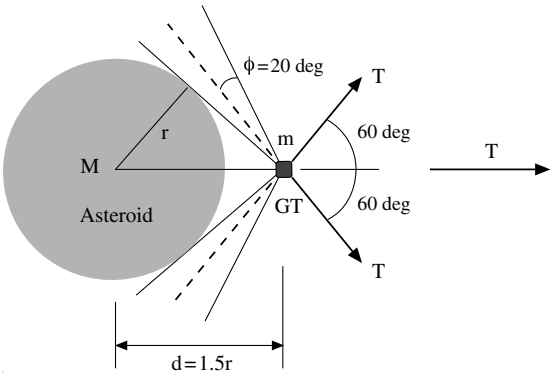

Fig. 1 A geometrical illustration of the GT concept for towing an asteroid [17].

spacecraft propelled by a nuclear-electric propulsion system is considered in [17], we consider here a 1000-kg spacecraft as an illustrative example applied to asteroid Apophis. To avoid exhaust plume impingement on the asteroid surface, two ion engines are properly tilted outward and the hovering distance is accordingly selected as $d = 1.5r$ and $\phi = 20$ deg. This illustrative combination yields an engine cant angle of 60 deg, and the two tilted thrusters (each with a thrust T) then produce a total towing thrust T, as illustrated in Fig. 1.

A simplified dynamic model for the target asteroid Apophis (ignoring its orbital motion) is

$$M\frac{\Delta V}{\Delta t} = \frac{GMm}{d^2} = T \tag{1}$$

or

$$\frac{\Delta V}{\Delta t} = \frac{Gm}{d^2} = \frac{T}{M} = A \tag{2}$$

where $G = 6.6695 \times 10^{-11}$ N $\cdot$ m^2/kg^2, $M = 4.6 \times 10^{10}$ kg, $m = 1000$ kg, $r = 160$ m, $d = 240$ m, $T = 0.05326$ N, $A = 1.1579 \times 10^{-9}$ mm/s^2 is the characteristic acceleration, and

$$\Delta V = A\Delta t \tag{3a}$$

$$\Delta X = \tfrac{1}{2}A(\Delta t)^2 \tag{3b}$$

where ΔV and ΔX are, respectively, the resulting velocity and position changes for the total towing period of Δt. For example, we have $\Delta V = 0.036$ mm/s and $\Delta X = 575$ m for $\Delta t =$ one year.

Including the orbital amplification effect (to be discussed in the Appendix), we have

$$\Delta V = 3A\Delta t \tag{4a}$$

$$\Delta X = \tfrac{3}{2}A(\Delta t)^2 \tag{4b}$$

Consequently, we have $\Delta V = 0.1$ mm/s and $\Delta X = 1.7$ km for one-year towing.

Including an additional coasting time of t_c, we have the total position change (i.e., the Earth miss distance) given by

$$\Delta X = \tfrac{3}{2}A\Delta t(\Delta t + 2t_c) \tag{5}$$

This deflection formula will be derived in the Appendix. Thus, one-year towing in 2026 with an additional coasting time of 3 years will cause a total position change of approximately 12 km in 2029, which is more than sufficient to safely move Apophis out of its 600-m keyhole in 2029.

The propellant amount required for maintaining a desired hovering altitude of 80 m can be estimated as

$$\Delta m_f = \frac{2T\Delta t}{g_o I_{\text{sp}}} \approx 0.3 \text{ kg per day} \approx 114 \text{ kg per year}$$

where $T = 0.053$ N, $g_o = 9.8$ m/s^2, and $I_{\text{sp}} = 3000$ s (assumed for typical ion engines).

Therefore, a 1000-kg GT spacecraft equipped with ion engines can be considered as a viable option for a pre-2029 deflection mission for Apophis. However, it is emphasized that a 1000-kg spacecraft, colliding with Apophis at a modest impact velocity of 10 km/s in 2026, will cause a much larger instantaneous velocity change of at least 0.22 mm/s for Apophis, resulting in an orbital deflection of 62 km in 2029. Such a higher-energy kinetic impactor approach may not be applicable to highly porous rubble-pile asteroids, whereas a GT spacecraft mission may need an additional large ΔV to rendezvous with a target asteroid. Consequently, further system-level tradeoffs on various practical issues, such as the total mission ΔV requirement, low-thrust gravity towing vs higher-energy kinetic impact, and asteroid dispersal/fragmentation concern, need to be performed in a future study, as recently assessed in [23].

IV. Multiple Gravity Tractors in Halo Orbits

A. Multiple Orbiting GTs Versus a Single Hovering GT with Canted Thrusters

A hovering GT in a static equilibrium standoff position requires canted thrusters to avoid plume impingement on the NEA surface. Consequently, McInnes [22] recently investigated a GT spacecraft flying in a displaced non-Keplerian orbit (also often called a halo orbit) for a possible fuel-efficient way of towing asteroids. However, a GT in a displaced orbit will require a much heavier spacecraft (about 2.8 times heavier than a single hovering GT) if its x-axis location is the same as the standoff distance d of a hovering GT. Or it will need to be placed much closer to the target asteroid (at about 59% of the standoff distance of a hovering GT) if it has the same mass as a hovering GT. Despite such drawbacks, a displaced orbit simply allows many GTs for towing a target asteroid. In this paper, a system of MGTs flying in halo orbits near a target asteroid is proposed as a viable near-term option for deflecting a certain class of NEAs such as asteroid 99942 Apophis or other highly porous rubble-pile asteroids.

The proposed MGT system may consist of several GTs in a primary halo orbit as well as in a secondary/backup halo orbit, as illustrated in Fig. 2. It has the following distinct performance and robustness improvements over a single hovering GT in a static equilibrium standoff position: a larger total ΔV capability, a multispacecraft redundancy, and a mission design flexibility with smaller satellites equipped with lower-risk propulsion systems. For example, instead of using a single large 2500-kg hovering GT spacecraft, we may employ an MGT system consisting of five (or more) small 500-kg satellites or two (or more) 2500-kg orbiting MGTs (if needed).

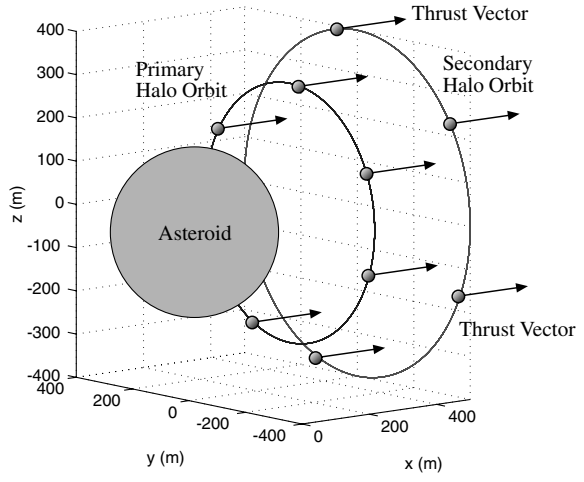

Fig. 2 A conceptual illustration of a system of MGTs in halo orbits.

B. Halo Orbit Dynamics and Control

A dynamic model of multiple gravity tractors towing a target asteroid is illustrated in Fig. 3. Using the Clohessy–Wiltshire–Hill equations of motion in astrodynamics [29], we can obtain the equations of motion of the asteroid-MGT system as

$$\ddot{x} = 2n\dot{y} + \sum_{i=1}^{N} Gm_i \frac{x_i - x}{r_i^3} \tag{6}$$

$$\ddot{y} = -2n\dot{x} + 3n^2 y + \sum_{i=1}^{N} Gm_i \frac{y_i - y}{r_i^3} \tag{7}$$

$$\ddot{z} = -n^2 z + \sum_{i=1}^{N} Gm_i \frac{z_i - z}{r_i^3} \tag{8}$$

$$\ddot{x}_i = 2n\dot{y}_i - GM\frac{x_i - x}{r_i^3} + \frac{T_i}{m_i} \tag{9}$$

$$\ddot{y}_i = -2n\dot{x}_i + 3n^2 y_2 - GM\frac{y_i - y}{r_i^3} \tag{10}$$

$$\ddot{z}_i = -n^2 z_i - GM\frac{z_i - z}{r_i^3} \tag{11}$$

where

$$r_i = \sqrt{(x_i - x)^2 + (y_i - y)^2 + (z_i - z)^2}$$

and (x, y, z) are the coordinates of the target asteroid with respect to an orbiting reference frame with the origin O, (x_i, y_i, z_i) are the coordinates of the ith GT spacecraft with respect to the reference frame origin O, T_i is the x-axis orbit control thrust of the ith GT spacecraft, G is the universal gravitational constant, M is the asteroid mass, m_i is the ith GT spacecraft mass, N is the total number of GTs, and n is the orbital rate of the reference frame. For simplicity, a circular heliocentric orbital motion of the target asteroid is considered here.

A simple x-axis control logic is assumed as

$$T_i = -K_p(x_i - x - d_i) - K_d(\dot{x}_i - \dot{x}) \tag{12}$$

where d_i is the desired x-axis location of the ith GT spacecraft. There is no need for y- and z-axes control forces for an ideal halo orbit case. However, in practice, the y- and z-axes orbit control would be required if the trajectory deviations from a desired halo orbit need to be corrected.

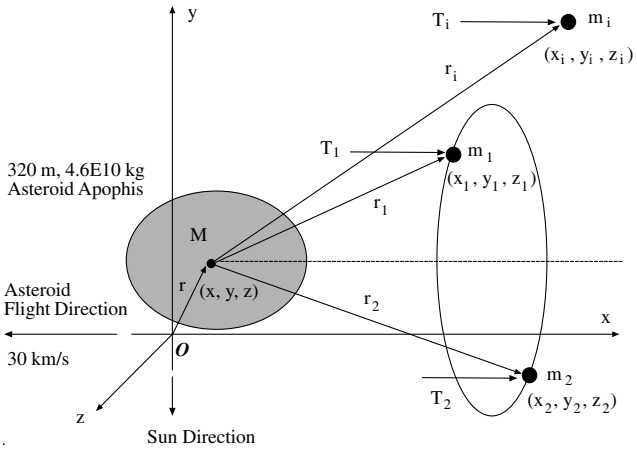

Fig. 3 A dynamic model of MGTs in halo orbits.

C. Ideal Circular Halo Orbit

Neglecting the effect of a slow orbital motion of the target asteroid, we obtain the following simplified model:

$$\ddot{x}_1 \approx -\frac{GMx_1}{r_1^3} + \frac{T_1}{m_1} \tag{13}$$

$$\ddot{y}_1 \approx -\frac{GMy_1}{r_1^3} \tag{14}$$

$$\ddot{z}_1 \approx -\frac{GMz_1}{r_1^3} \tag{15}$$

where

$$r_1 = \sqrt{x_1^2 + y_1^2 + z_1^2}$$

To maintain a halo orbit at a fixed displacement of x_1, the x-axis thrust force must counter the gravity force as

$$T_1 = \frac{GMm_1x_1}{r_1^3}$$

Assuming that

$$y_1(t) = A\cos(\Omega t + \phi) \tag{16a}$$

$$z_1(t) = A\sin(\Omega t + \phi) \tag{16b}$$

where A is the halo orbit amplitude and Ω is the halo orbit frequency, we simply find the following constraints:

$$y_1^2 + z_1^2 = A^2 \tag{17a}$$

$$\dot{y}_1^2 + \dot{z}_1 = (A\Omega)^2 \tag{17b}$$

where

$$\Omega = \sqrt{\frac{GM}{r_1^3}} \tag{18}$$

A set of proper initial conditions for a halo orbit insertion is given by

$$x_1(0) = d_1 = \text{halo orbit x-axis displacement}$$

$$y_1(0) = \pm A = \text{halo orbit amplitud}e \qquad z_1(0) = 0$$

$$\dot{x}_1(0) = \dot{y}_1(0) = 0$$

$$\dot{z}_1(0) = \pm A\Omega = \pm A\sqrt{\frac{GM}{r_1^3}} = \text{halo orbit insertion}\Delta V$$

D. Numerical Simulations of Illustrative Cases

Numerical simulation conditions for two illustrative cases for towing asteroid Apophis are summarized in Table 2. A fictional mission scenario of employing two halo orbits (primary and secondary) is considered for both cases, and a single 1000-kg GT is placed in each halo orbit. Case 1 corresponds to an ideal situation without any modeling uncertainty. Case 2 represents a more realistic situation with a 1-deg thrust vector misalignment, halo orbit insertion errors, and a target asteroid with a spin period of 16 h and a center-of-mass/center-of-gravity offset of 10 m. An ideal exhaust plume model of a uniform cone with a half-angle of 20 deg [17,18,22] is also assumed. No y- and z-axes orbit control is used for both cases. However, in practice, the y- and z-axes control will be required, especially for the MGTs placed in a low-altitude primary halo orbit if the trajectory deviations from a desired periodic halo orbit, caused by a tumbling motion of an irregularly shaped asteroid, are not acceptable.

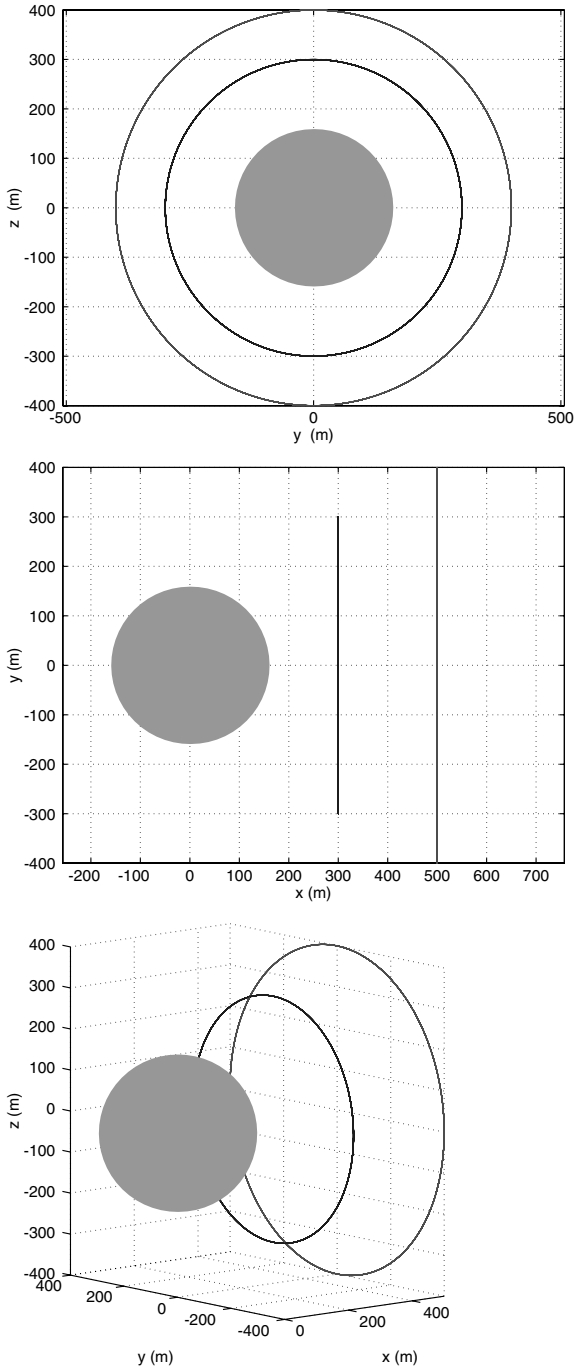

Fig. 4 Halo orbit control simulation for case 1.

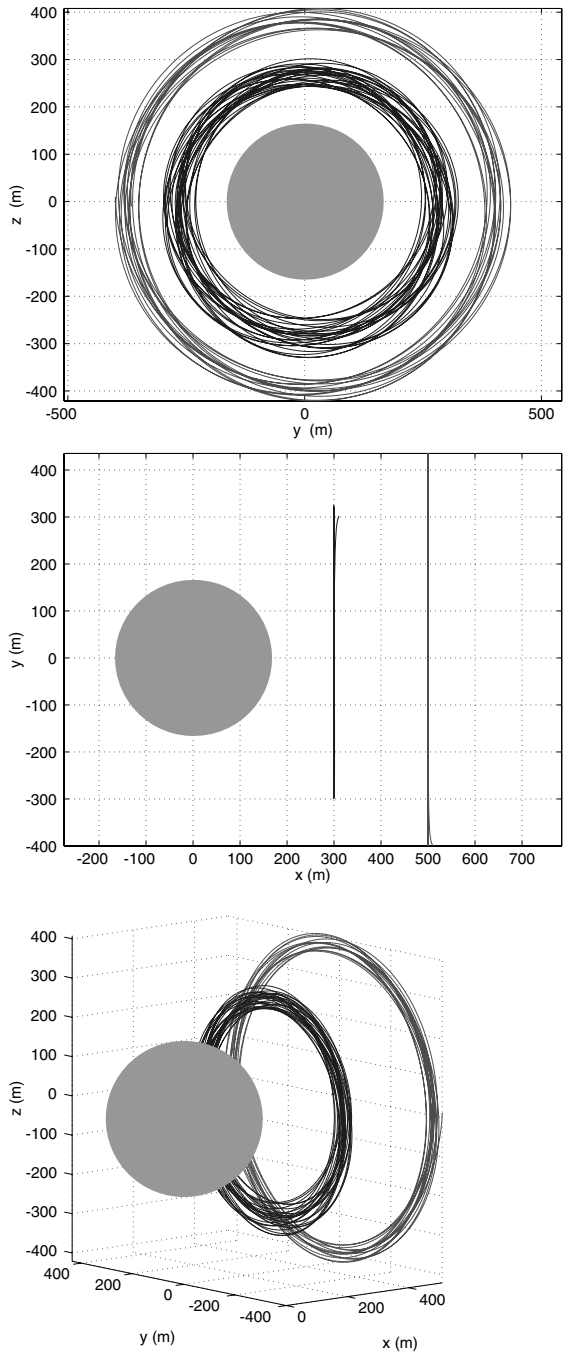

Fig. 5 Halo orbit control simulation for case 2.

As can be seen in Fig. 4 for case 1, two ideal circular halo orbits are achieved using the simple control logic as described by Eq. (12). Simulation results shown in Figs. 5–7 demonstrate that near-circular, but nonperiodic, halo orbits can also be achieved for case 2. The 1000-kg GT spacecraft may be replaced by two 500-kg satellites by properly placing them in a halo orbit. The resulting asteroid ΔV (Fig. 7) can be increased, if needed, by simply adding more GTs in halo orbits. However, a further system-level tradeoff study is needed for overall mission design tradeoffs, propulsion system selection tradeoffs, halo orbit insertion/maintenance, high-fidelity dynamic modeling of highly asymmetric asteroids, orbit control design, and simulations.

V. Hovering Solar-Sail Gravity Tractor

A. Baseline Solar-Sail Gravity Tractor for Asteroid Apophis

Using the same physical principle of employing the mutual gravitational force between a hovering spacecraft and a target asteroid as a towline, we may choose solar sails/reflectors rather than nuclear-electric propulsion systems to produce the required continuous low-thrust towing force [21].

For a solar sailing kinetic impactor mission, proposed in [13–16], its large lightweight solar sail will be deployed at the beginning of an interplanetary solar sailing flight toward a target asteroid and the impactor spacecraft will be separated from the solar sail before impacting a target asteroid. For a solar sail gravity tractor (SSGT) spacecraft mission, its large solar sail will be deployed after completing a rendezvous with a target asteroid, but its large solar sail is not required to be lightweight.

As an example, for Apophis, we may need a 2500-kg SSGT spacecraft, equipped with a 90×90 m solar sail of a 0.03-N solar thrust with a 35-deg sun angle, as illustrated in Fig. 8. Such a particular hovering position with an offset angle of $\theta = 55$ deg from an asteroid's flight direction is necessary because of the 35-deg sun-angle requirement of a typical solar sail/collector to produce a maximum solar pressure thrust. A larger (2500-kg) SSGT, compared

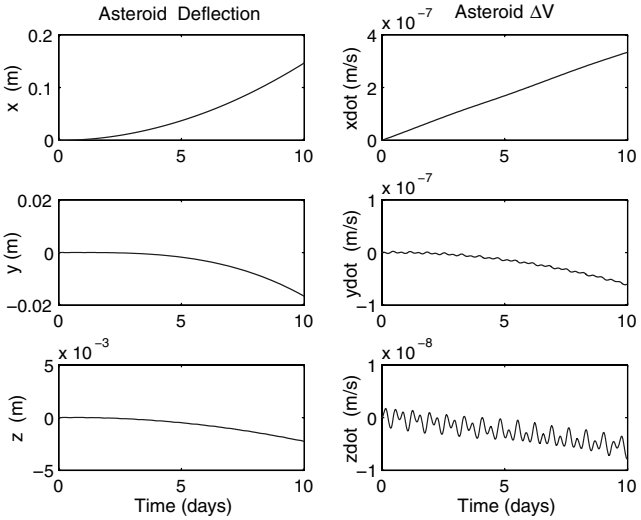

Fig. 6 Halo orbit control simulation for case 2 (continued).

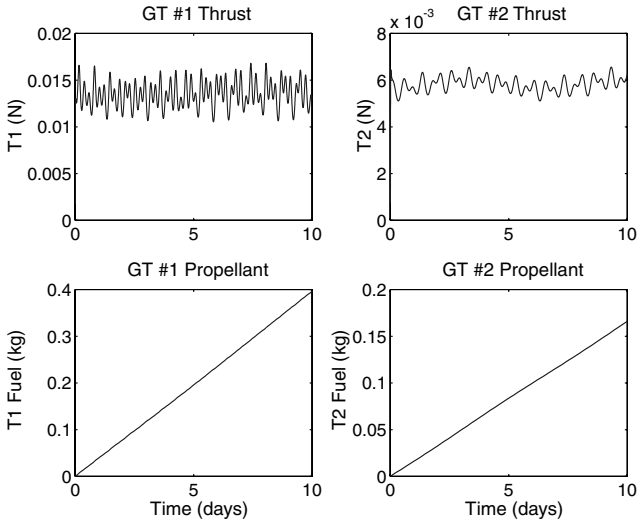

Fig. 7 Halo orbit control simulation for case 2 (continued).

with a 1000-kg GT equipped with ion engines, is to be placed at a higher altitude of 350 m because of its large solar sail/collector. This 2500-kg SSGT produces an along-track acceleration of $A_x = 3.8 \times 10^{-10}$ mm/s^2 and a radial acceleration of $A_y = 5.4 \times 10^{-10}$ mm/s^2 of the target asteroid Apophis. However, its radial acceleration component A_y has a negligible effect on the asteroid deflection. This fact can be considered as an inherent drawback of the SSGT, although a solar sail/reflector is a propellantless propulsion system.

A 5-year towing of Apophis using this 2500-kg SSGT spacecraft and a 3-year coasting time will result in an orbital deflection of 30 km in 2029, which is more than sufficient to move Apophis out of its 600-m keyhole. However, the SSGT spacecraft is intended to be employed for a much longer mission lifetime (greater than 5 years) to fully exploit its propellantless ΔV capability, which is its only advantage over a GT equipped with ion engines.

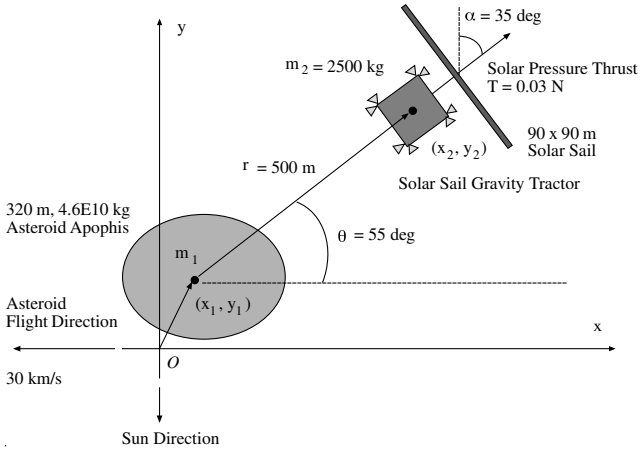

Fig. 8 A simplified dynamic model for hovering control analysis of a SSGT spacecraft.

B. Dynamic Modeling and Hovering Control

A simple planar model of the hovering dynamics of an SSGT spacecraft towing a target asteroid is illustrated in Fig. 8. Using the Clohessy–Wiltshire–Hill equations of motion [29], we can obtain the orbital equations of motion of the asteroid-SSGT system orbiting around the sun as follows:

$$\ddot{x}_1 = 2n\dot{y}_1 + Gm_2\frac{x_2 - x_1}{r^3} \tag{19}$$

$$\ddot{y}_1 = -2n\dot{x}_1 + 3n^2 y_1 + Gm_2\frac{y_2 - y_1}{r^3} \tag{20}$$

$$\ddot{x}_2 = 2n\dot{y}_2 - Gm_1\frac{x_2 - x_1}{r^3} + \frac{1}{m_2}(T_x + F_x) \tag{21}$$

$$\ddot{y}_2 = -2n\dot{x}_2 + 3n^2 y_2 - Gm_1\frac{y_2 - y_1}{r^3} + \frac{1}{m_2}(T_y + F_y) \tag{22}$$

$$r = \sqrt{(x_2 - x_1)^2 + (y_2 - y_1)^2}$$

where (x_1, y_1) are the coordinates of the target asteroid with respect to an orbiting reference frame, (x_2, y_2) are the coordinates of the SSGT spacecraft, (T_x, T_y) are the solar pressure thrust components, (F_x, F_y) are the control thrust components, G is the universal gravitational constant, m_1 is the asteroid mass, m_2 is the SSGT spacecraft mass, and n is the orbital rate of the reference frame. For simplicity, a circular orbital motion of the reference frame is considered here. The eccentric orbital effect of a target asteroid will be discussed in the Appendix.

Preliminary hovering control logic is considered as follows:

$$\tan\theta = \frac{y_2 - y_1}{x_2 - x_1}, \qquad \alpha = \frac{\pi}{2} - \theta,$$

$$T_x = T_o \cos^2\alpha \sin\alpha,$$

$$T_y = T_o \cos^2\alpha \cos\alpha,$$

$$x = x_2 - x_1 = r\cos\theta,$$

$$y = y_2 - y_1 = r\sin\theta,$$

$$F_x = -K_p(x - x_c) - K_d\dot{x},$$

$$F_y = -K_p(y - y_c) - K_d\dot{y}$$

$$\text{if } |F_x| > F_{\max}, \qquad F_x = \text{sgn}(F_x)F_{\max}$$

$$\text{if } |F_y| > F\max, \qquad F_y = \text{sgn}(F_y)F_{\max}$$

$$\text{if } |x - x_c| < \epsilon_x, \qquad F_x = 0$$

$$\text{if } |y - y_c| < \epsilon_y, \qquad F_y = 0$$

where $T_o = 0.045$ N for a 90-m solar sail at 1 AU, $F_{\max} = 0.05$ N, $\epsilon_x = \epsilon_y = 10$ m, and (x_c, y_c) is the desired hovering position command. For simplicity, electric thrusters with a maximum thrust of 0.05 N and a specific impulse of 3000 s are considered for the hovering control of SSGT spacecraft.

Hovering control simulation results are shown in Figs. 9–13 for a 2500-kg SSGT spacecraft. For these simulations, a spin period of 16 h and a center-of-mass/center-of-gravity offset of 10 m is assumed. As can be estimated from Fig. 13, less than 3-kg propellant per year (worst case) may be needed for a 2500-kg SSGT spacecraft to hover above a target asteroid with its uncertain gravitational environment. Any undesirable cyclic thruster firings can be easily eliminated by employing a cyclic-disturbance rejection control scheme to reduce the hovering control propellant consumption (if needed). A more rigorous dynamic model of the gravitational field of a slowly rotating irregularly shaped asteroid needs to be employed for the detailed hovering control design and high-fidelity simulations.

C. Gravity Gradient Torque Estimation

The pitch-axis attitude dynamic model of a large 90-m SSGT spacecraft hovering over Apophis is simply described by

$$I_2\ddot{\theta}_2 - \frac{3\mu}{R^3}(I_3 - I_1)\theta_2 = 0 \tag{23}$$

where $\mu = GM = 3\ \mathrm{N}\cdot\mathrm{m}^2/\mathrm{kg}$ ($G = 6.6695 \times 10^{-11}\ \mathrm{N}\cdot\mathrm{m}^2/\mathrm{kg}^2$, $M = 4.6 \times 10^{10}$ kg), $I_1 = I_2 = 300{,}000\ \mathrm{kg}\cdot\mathrm{m}^2$, $I_3 = 600{,}000\ \mathrm{kg}\cdot\mathrm{m}^2$, and $R = 500$ m. For this case, we have

$$I_2\ddot{\theta}_2 - 0.02\theta_2 = 0 \tag{24}$$

The peak primary gravity gradient torque can be estimated as $0.01\ \mathrm{N}\cdot\mathrm{m}$ for an assumed peak pitch-attitude error of 30 deg. Such a small peak gravity gradient disturbance torque is not of practical concern for a three-axis stabilized SSGT spacecraft. However, the coupled attitude and hovering control problem of such a large solar sail spacecraft needs a detailed study by expanding upon the recent progresses in solar sail attitude control as described in [30–32] and also using a complex model of a large hovering GT spacecraft near an asteroid described in [33].

D. Technology Readiness Level of Solar Sails

Compared with the Technology Readiness Level (TRL) of ion engines, the current TRL of solar sails is extremely low. However, the recent advances in lightweight deployable booms, ultralight-weight sail films, and small satellite technologies are spurring a

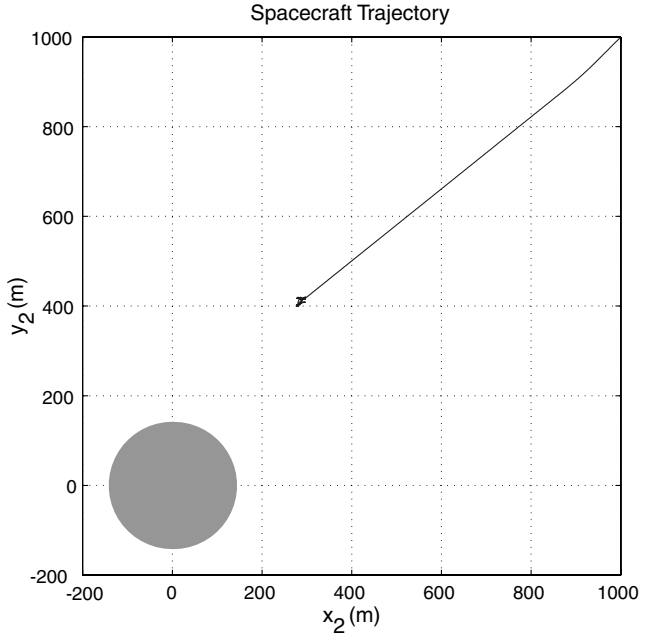

Fig. 9 Hovering control simulation results for the SSGT; starting point at $(x, y) = (1000, 1000)$ m and a desired hovering point $(x, y) = (286, 409)$ m.

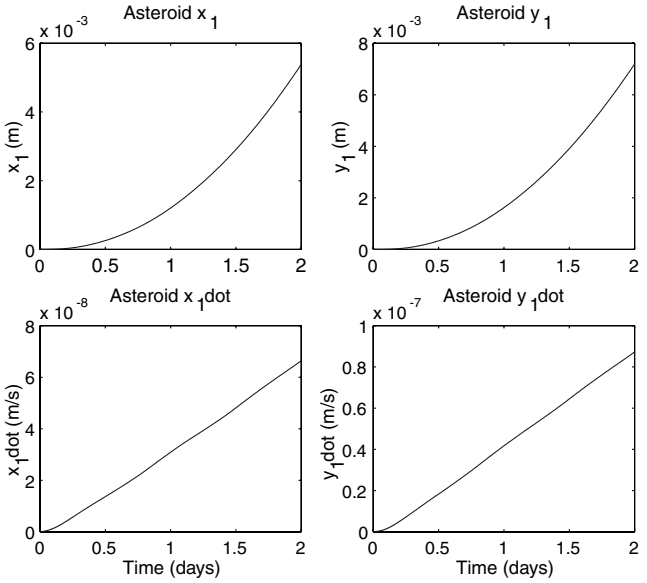

Fig. 10 Hovering control simulation results for the SSGT (continued).

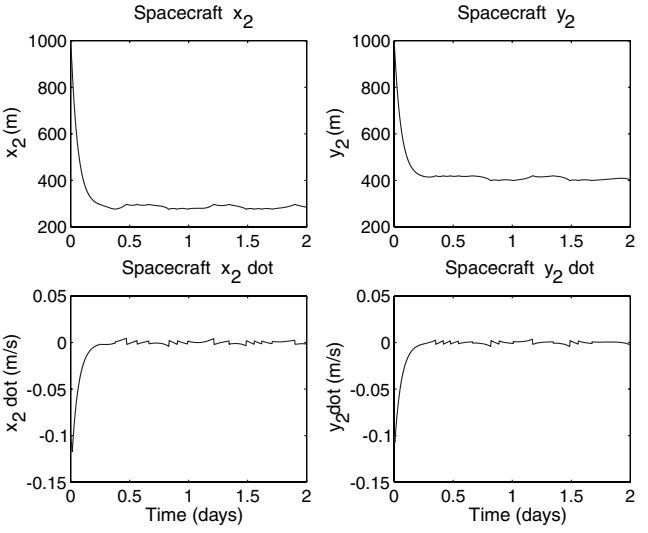

Fig. 11 Hovering control simulation results for the SSGT (continued).

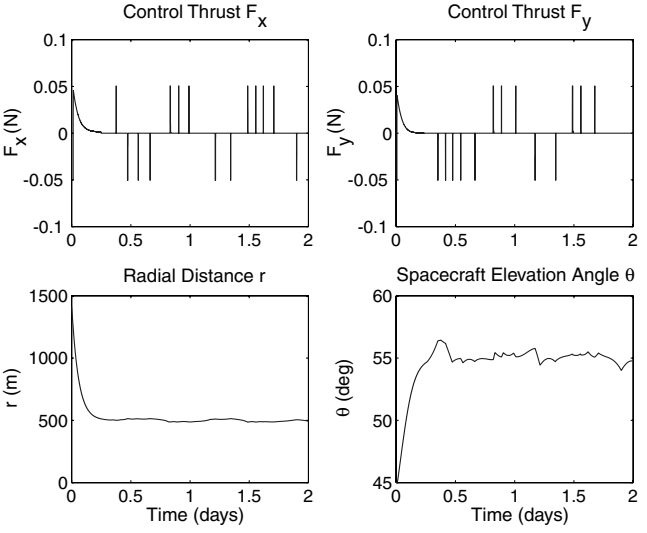

Fig. 12 Hovering control simulation results for the SSGT (continued).

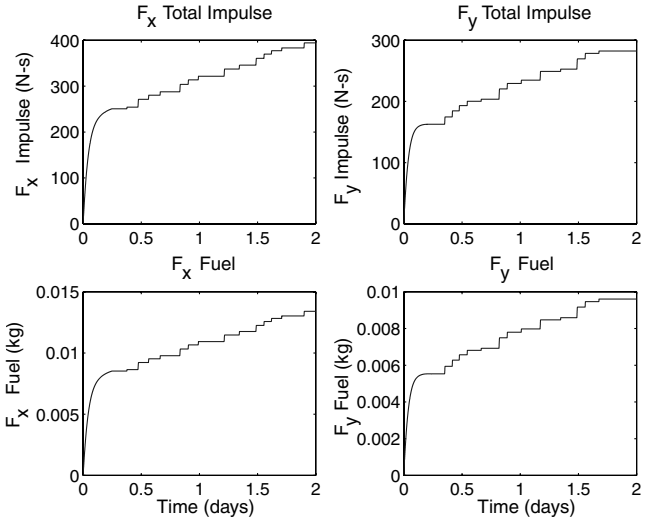

Fig. 13 Hovering control simulation results for the SSGT (continued).

renewed interest in solar sailing and the missions it enables. Consequently, various near-term solar sailing missions and the associated technologies are being developed [34,35]. A 20-m solar sail ground-validation project of NASA's In-Space Propulsion Technology Program was successfully completed in 2005 [36,37]. A space flight experiment of the 30-m, 105-kg Cosmos 1 solar sail spacecraft was attempted by The Planetary Society on 21 June 2005. Because of a boost rocket failure, the Cosmos 1 solar sail project did not achieve its mission goal of demonstrating the first controlled solar sail flight. A 40-m solar sail has been considered by NASA and industries for a possible flight validation experiment. A 160-m solar sail will be required for NASA's Solar Polar Imager mission, which is one of the Sun–Earth Connections solar sail roadmap missions currently envisioned by NASA [38]. However, it seems that a 100-m class solar sail required to propel the SSGT spacecraft will not be available in the near future, and the deployment and control of such a large solar sail in space will not be a trivial task.

VI. Conclusions

Rather than employing nuclear explosions or kinetic impactors, we may have to use the slow-pull gravity tractor approach for deflecting a certain class of near-Earth asteroids such as asteroid 99942 Apophis or other highly porous rubble-pile asteroids. A system of multiple gravity tractors in halo orbits, with its inherent multispacecraft redundancy advantage, can be a viable near-term option for towing a certain class of asteroids that may not require high-energy deflection techniques. This paper has also demonstrated the usefulness of the modified Clohessy–Wiltshire–Hill equations for the preliminary control analysis and simulation of the gravity tractor spacecraft for towing asteroids.

Appendix: Asteroid Deflection Dynamics

In this Appendix, we employ Clohessy–Wiltshire–Hill equations [29] to discuss the fundamentals of asteroid deflection dynamics discussed in [39–41]. The long-term effect of a target asteroid's orbital eccentricity on asteroid deflection is also discussed using simulation results.

I. Orbital Amplification Effect on the Miss Distance

Consider the Clohessy–Wiltshire–Hill equations of motion of a target asteroid (in an assumed heliocentric circular orbit) described by

$$\ddot{x} = 2n\dot{y} + A_x \tag{A1}$$

$$\ddot{y} = -2n\dot{x} + 3n^2 y + A_y \tag{A2}$$

where (x, y) are the coordinates of an asteroid with respect to a circular orbit reference frame shown in Fig. 8 and (A_x, A_y) are the gravitational-towing acceleration components acting on the asteroid. The out-of-plane motion is not considered here. A simple case with $A_x = A =$ constant and $A_y = 0$ is further assumed here without loss of generality because the asteroid deflection effect of a nonzero A_y is practically negligible. For an asteroid towed by a single hovering GT, we have $A_y \equiv 0$.

Integrating the x-axis equation, we obtain

$$\dot{x} = \dot{x}(0) + 2ny + At \tag{A3}$$

where $\dot{x}(0)$ denotes the along-track velocity at $t = 0^-$. All other initial conditions will be ignored here. For a kinetic-energy impactor problem, the initial impact ΔV along the x-axis direction becomes $\dot{x}(0)$.

Substituting Eq. (A3) into the y-axis equation, we obtain

$$\ddot{y} + n^2 y = -2n\dot{x}(0) - 2nAt \tag{A4}$$

Its solution can be found as

$$y(t) = -\frac{2}{n}\dot{x}(0)(1 - \cos nt) - \frac{2}{n}A\left(t - \frac{1}{n}\sin nt\right) \tag{A5}$$

and

$$\dot{y}(t) = -2\dot{x}(0)\sin nt - \frac{2}{n}A(1 - \cos nt) \tag{A6}$$

We then obtain

$$\dot{x}(t) = -\dot{x}(0)(3 - 4\cos nt) - 3At + \frac{4}{n}A\sin nt \tag{A7}$$

which can be integrated as

$$x(t) = -\dot{x}(0)\left(3t - \frac{4}{n}\sin nt\right) - \frac{3}{2}At^2 + \frac{4}{n^2}A(1 - \cos nt) \tag{A8a}$$

$$\approx -3\dot{x}(0)t - \tfrac{3}{2}At^2 \quad \text{for large } t \tag{A8b}$$

The orbital amplification factor of 3 can be seen from the preceding equation. Note that the positive values of $\dot{x}(0)$ and A slow down the asteroid and reduce its orbital energy. Consequently, its along-track position becomes negative (i.e., ahead of its unperturbed virtual position in a circular reference orbit).

Consider an asteroid with the accelerated towing time of t_a and the additional coasting time of t_c. It is assumed that $\dot{x}(0) = 0$ here. A new set of initial conditions at the end of the towing period become

$$x_0 = -\frac{3}{2}At_a^2 + \frac{4}{n^2}A(1 - \cos nt_a) \qquad \dot{x}_0 = -3At_a + \frac{4}{n}A\sin nt_a,$$
$$y_0 = -\frac{2}{n}A\left(t_a - \frac{1}{n}\sin nt_a\right), \qquad \dot{y}_0 = -\frac{2}{n}A(1 - \cos nt_a)$$

The final position changes at the end of the coasting phase can then be found as

$$\Delta x = x_0 + (6ny_0 - 3\dot{x}_0)t_c + \frac{2\dot{y}_0}{n}(1 - \cos nt_c) + \left(\frac{4\dot{x}_0}{n} - 6y_0\right)\sin nt_c \tag{A9}$$

$$\Delta y = 4y_0 - \frac{2\dot{x}_0}{n} + \left(\frac{2\dot{x}_0}{n} - 3y_0\right)\cos nt_c + \frac{\dot{y}_0}{n}\sin nt_c \tag{A10}$$

Substituting the initial conditions into Eq. (A9), we obtain

$$\Delta x \approx -\tfrac{3}{2}At_a(t_a + 2t_c) \tag{A11}$$

which is the low-thrust deflection formula discussed in [39–41] using different approaches. Note that $\Delta y \approx 0$ compared with Δx.

Equation (A11) can be rewritten as

$$\Delta x = -(\tfrac{3}{2}At_a^2 + \Delta V t_c) \quad \text{where} \quad \Delta V = 3At_a \tag{A12}$$

Note that Δx is caused by various initial conditions including $\dot{x}_0$ and y_0 as can be seen in Eq. (A9). Such a combined effect of $\dot{x}_0$ and y_0 results in the term $\Delta V t_c$ (not $3\Delta V t_c$ as one might expect) in Eq. (A12).

For an asteroid in an eccentric orbit colliding with the Earth, we have

$$V = V_\oplus \sqrt{2 - \frac{r_\oplus}{a}} \tag{A13}$$

$$e^2 = (\lambda - 1)^2 \cos^2\gamma + \sin^2\gamma \tag{A14}$$

where V is its heliocentric velocity at an impact point, a is its semimajor axis, e is its eccentricity, $r_\oplus = 1$ AU $= 1.496 \times 10^8$ km, $V_\oplus = 29.784$ km/s, γ is the intersection angle between $\mathbf{V}$ and $\mathbf{V}_\oplus$, and $\lambda = (V/V_\oplus)^2$. The heliocentric elevation angle γ is also called the flight-path angle.

As illustrated in Fig. 14 for a case with $a \approx r_\oplus$, we have

$$V \approx V_\oplus, \qquad e \approx \sin\gamma, \qquad d = \Delta x \cos(\gamma/2)$$

where d is the approach distance (also called the b-plane miss distance). The impact parameter b, which defines the radius of a collision cross section, is given by

$$b = R_\oplus \sqrt{1 + \frac{V_e^2}{V_\infty^2}} \tag{A15}$$

where $R_\oplus$ is the radius of the Earth (6378 km/s), $V_e = \sqrt{2\mu_\oplus / R_\oplus}$ is the escape velocity from the surface of the Earth (11.18 km/s), and V_∞ is the hyperbolic approach velocity. To avoid an impact, we simply need $d > b$.

For a somewhat unusual case of a near-head-on collision of an asteroid with the Earth, we can obtain

$$d = \Delta x \sin(\gamma/2) \approx -\frac{3e}{4} A t_a (t_a + 2t_c)$$

This formula was previously presented in [41] without mentioning that this formula is only applicable to a retrograde (head-on) collision case. In practice, it will be extremely difficult to deflect a NEO that is in a head-on collision orbital path toward the Earth, also evidenced in this formula.

For an impulsive ΔV along the x-axis direction, the resulting deflection Δx after a coasting time of t_c is simply given by

$$\Delta x = -3\Delta V tc \tag{A16}$$

For a kinetic impactor approach, ΔV can be estimated as

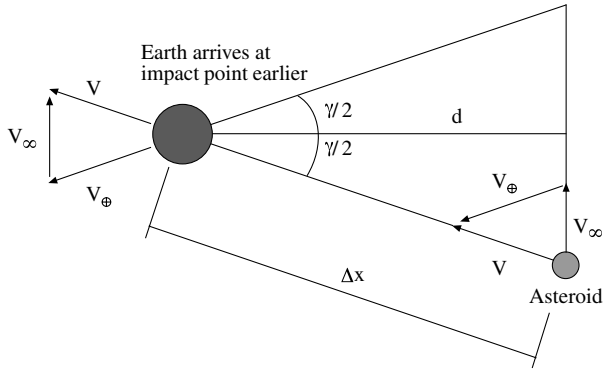

Fig. 14 Asteroid deflection geometry for a case with $a \approx 1$ AU.

$$\Delta V \approx \beta \frac{m}{M+m} U \approx \beta \frac{m}{M} U \tag{A17}$$

where β is the impact efficiency factor, m is the impactor mass, M is the target asteroid mass, and U is the relative impact velocity.

For asteroid Apophis, towed by an SSGT spacecraft, with an assumed circular orbital period of 323 days ($n = 2.2515 \times 10^{-7}$ rad/s), a low-thrust acceleration of $A_x = 3.8284 \times 10^{-10}$ mm/s^2, $A_y = 5.4667 \times 10^{-10}$ mm/s^2, $t_a = 5$ years, and $t_c = 3$ years, the final position change Δx can then be estimated as -30 km, as can also be noticed in Fig. 15.

II. Eccentricity Effect on the Miss Distance

Consider the Clohessy–Wiltshire–Hill equations of motion of a target asteroid in an elliptical reference orbit as described by

$$\ddot{x} = 2\dot{\theta}\dot{y} + \ddot{\theta} y + \dot{\theta}^2 x - \frac{\mu}{r^3} x + A_x \tag{A18}$$

$$\ddot{y} = -2\dot{\theta}\dot{x} - \ddot{\theta} x + \dot{\theta}^2 y + \frac{2\mu}{r^3} y + A_y \tag{A19}$$

$$\ddot{r} = r\dot{\theta}^2 - \frac{\mu}{r^2} \tag{A20}$$

$$\ddot{\theta} = -\frac{2\dot{r}\dot{\theta}}{r} \tag{A21}$$

where (x, y) are the relative coordinates of the target asteroid with respect to a reference point of its nominal elliptical orbit, r is the radial distance of the reference orbit from the sun, θ is the true anomaly, and μ is the gravitational parameter of the sun. Furthermore, we have

$$r = \frac{p}{1 + e\cos\theta} \tag{A22a}$$

$$\dot{r} = \sqrt{\mu/p}(e \sin\theta) \tag{A22b}$$

$$\dot{\theta} = \sqrt{\mu/p3}(1 + e\cos\theta)^2 \tag{A22c}$$

where $p = a(1 - e^2)$.

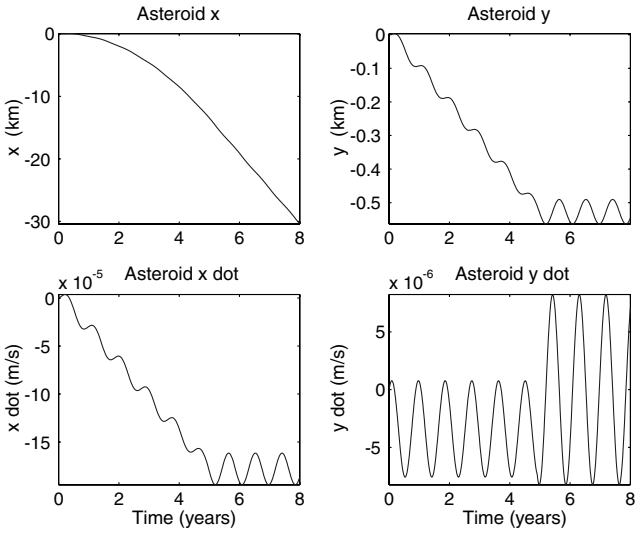

Fig. 15 Long-term simulation for Apophis assuming $e = 0$ (towed by a 2500-kg SSGT).

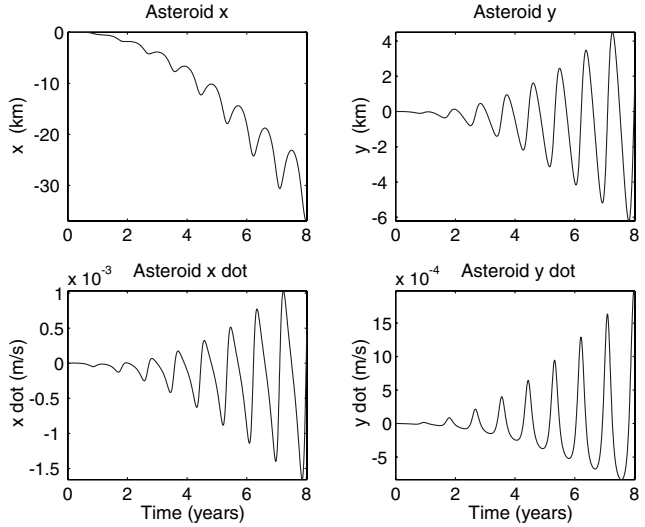

Fig. 16 Long-term simulation for Apophis with $e = 0.19$ (towed by a 2500-kg SSGT).

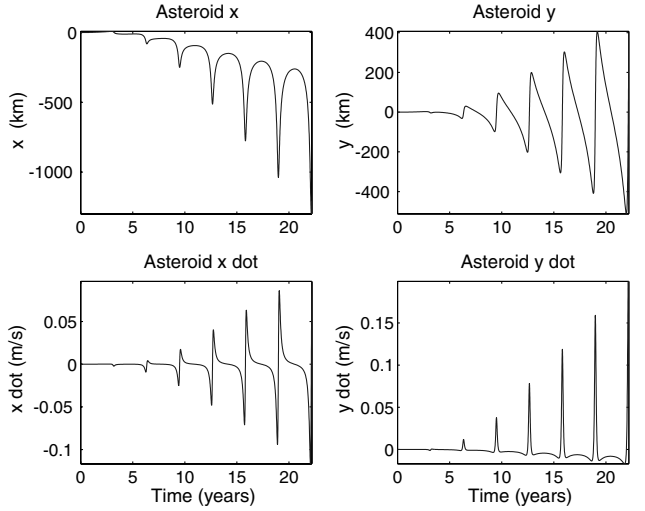

Fig. 17 Long-term simulation for a fictional 200-m asteroid [14] with $e = 0.6498$ (towed by a 2500-kg SSGT).

For Apophis with $e = 0.19$, a low-thrust acceleration of $A_x = 3.8284 \times 10^{-10}$ mm/s^2, $A_y = 5.4667 \times 10^{-10}$ mm/s^2, $t_a = 5$ years, and $t_c = 3$ years, the eccentricity effect on the nonsecular terms is evident in Fig. 16, compared with Fig. 15 for the same case but with $e = 0$.

To further examine the eccentricity effect, consider a fictional 200-m asteroid [14], towed by an SSGT spacecraft, with $M = 1.1 \times 10^{10}$ kg, $a = 2.1537$ AU, $e = 0.6498$, $A_x = 1.76 \times 10^{-9}$ mm/s^2, and $A_y = 2.51 \times 10^{-9}$ mm/s^2. Simulation results for $t_a = 10$ years and $t_c = 12$ years are shown in Fig. 17. The significant effect of a large eccentricity ($e = 0.6498$) is evident in Fig. 17.

Table 2 Simulation conditions for the two illustrative cases applied to asteroid Apophis

	Case 1 (ideal)		Case 2 (realistic)	
	GT no. 1	GT no. 2	GT no. 1	GT no. 2
m_i, kg	1000	1000	1000	1000
d_i, m	300	500	300	500
$x_i(0)$, m	300	500	310	510
$y_i(0)$, m	300	−400	300	−400
$z_i(0)$, m	0	0	10	10
$\dot{x}_i(0)$, m/s	0	0	0.001	0.001
$\dot{y}_i(0)$, m/s	0	0	0.001	0.001
$\dot{z}_i(0)$, m/s	0.0601	−0.0432	0.0601	−0.0432

References

[1] Brown, P., Spalding, R. E., ReVelle, D. O., Tagliaferri, E., and Worden, S. P., "The Flux of Small Near-Earth Objects Colliding with the Earth," *Nature*, Vol. 420, 2002, pp. 294–296. doi:10.1038/nature01238

[2] Cheng, A., "Near Earth Asteroid Rendezvous: Mission Summary," *Asteroids III*, Univ. of Arizona Press, Tucson, AZ, 2002, pp. 351–366.

[3] Ahrens, T. J., and Harris, A. W., "Deflection and Fragmentation of Near-Earth Asteroids," *Hazards Due to Comets and Asteroids*, edited by Gehrels, T., Univ. of Arizona Press, Tucson, AZ, 1994, pp. 897–927.

[4] Belton, M., Morgan, T., Samarasinha, N., and Yeomans, D. (ed.), *Mitigation of Hazardous Comets and Asteroids*, Cambridge Univ. Press, Cambridge, England, U.K., 2005.

[5] Gold, R. E., "SHIELD: A Comprehensive Earth Protection System," NASA, Mar. 2007.

[6] Schweickart, R., Lu, E., Hut, P., and Chapman, C., "The Asteroid Tugboat," *Scientific American*, Vol. 289, No. 5, Nov. 2003, pp. 54–61.

[7] Adams, R. B., Alexander, R., Bonometti, J., Chapman, J., Fincher, S., Hopkins, R., Kalkstein, M., Polsgrove, T., Statham, G., and White, S., "Survey of Technologies Relevant to Defense from Near-Earth Objects," NASA Marshall Space Flight Center, NASA-TP-2004-213089, Huntsville, AL, July 2004.

[8] Richardson, D. C., Leinhardt, Z. M., Melosh, H. J., Bottke, W. F., Jr.,, and Asphaug, E., "Gravitational Aggregates: Evidence and Evolution," *Asteroids III*, Univ. of Arizona Press, Tucson, AZ, 2002, pp. 501–515.

[9] Hall, C. D., and Ross, I. M., "Dynamics and Control Problems in the Deflection of Near-Earth Objects," AAS/AIAA Space Flight Mechanics Conference, American Astronautical Society Paper 97-640, Aug. 1997.

[10] Park, S.-Y., and Ross, I. M., "Two-Body Optimization for Deflecting Earth-Crossing Asteroids," *Journal of Guidance, Control, and Dynamics*, Vol. 22, No. 3, 1999, pp. 415–420.

[11] Conway, B. A.,"Near-Optimal Deflection of Earth Approaching Asteroids," *Journal of Guidance, Control, and Dynamics*, Vol. 24, No. 5, 2001, pp. 1035–1037.

[12] Izzo, D., Negueruela, C., Ongaro, F., and Walker, R., "Strategies for Near Earth Object Impact Hazard Mitigation," 15th AAS/AIAA Space Flight Mechanics Conference, Copper Mountain, CO, American Astronautical Society Paper 05-147, Jan. 2005.

[13] McInnes, C. R., "Deflection of Near-Earth Asteroids by Kinetic Energy Impacts from Retrograde Orbits," *Planetary and Space Science*, Vol. 52, No. 7, 2004, pp. 587–590. doi:10.1016/j.pss.2003.12.010

[14] Wie, B., "Solar Sailing Kinetic Energy Interceptor Mission for Impacting and Deflecting Near-Earth Asteroids," 41st AIAA Joint Propulsion Conference and Exhibit, AIAA Paper 2005-3725, Tucson, AZ, July 2005.

[15] Dachwald, B., and Wie, B., "Solar Sail Kinetic Energy Impactor Trajectory Optimization for an Asteroid-Deflection Mission," *Journal of Spacecraft and Rockets*, Vol. 44, No. 4, 2007, pp. 755–764. doi:10.2514/1.22586

[16] Dachwald, B., Kahle, R., and Wie, B., "Solar Sailing KEI Mission Design Tradeoffs for Impacting and Deflecting Asteroid 99942 Apophis," AIAA/AAS Astrodynamics Specialists Conference, AIAA Paper 2006-6178, Keystone, CO, Aug. 2006.

[17] Lu, E., and Love, S., "Gravitational Tractor for Towing Asteroids," *Nature*, Vol. 438, Nov. 2005, pp. 177–178. doi:10.1038/438177a

[18] Schweickart, R., Chapman, C., Durda, D., and Hut, P., "Threat Mitigation: The Gravity Tractor," NASA Workshop on NEO Detection, Characterization, and Threat Mitigation, Vail, CO, NASA White Paper No. 042, June 2006.

[19] Shkadov. L. M., "Possibility of Controlling Solar System Motion in the Galaxy, 38th International Astronautical Federation Congress, Brighton, England, U.K., International Academy of Astronautics Paper 87-613, Oct. 1987.

[20] McInnes, C. R., "Astronomical Engineering Revisited: Planetary Orbit Modification Using Solar Radiation Pressure," *Astrophysics and Space Science*, Vol. 282, No. 4, 2002, pp. 765–772. doi:10.1023/A:1021178603836

[21] Wie, B., "Hovering Control of a Solar Sail Gravity Tractor Spacecraft for Asteroid Deflection," AAS/AIAA Space Flight Mechanics Meeting,

Sedona, AZ, American Astronautical Society Paper 07–145, Jan.–Feb. 2007.
[22] McInnes, C. R., "Near Earth Object Orbit Modification Using Gravitational Coupling," *Journal of Guidance, Control, and Dynamics*, Vol. 30, No. 3, 2007, pp. 870–872.
[23] "2006 Near-Earth Object Survey and Deflection Study: Final Report," NASA, Mar. 2007.
[24] Kahle, R., Hahn, G., and Kührt, E., "Optimal Deflection of NEOs in Route of Collision with the Earth," *Icarus*, Vol. 182, No. 2, June 2006, pp. 482–488.
doi:10.1016/j.icarus.2006.01.005
[25] Chodas, P., and Yeomans, D., "Predicting Close Approaches and Estimating Impact Probabilities for Near-Earth Objects," AAS/AIAA Astrodynamics Specialists Conference, Girdwood, AK, American Astronautical Society Paper 99-462, Aug. 1999.
[26] Valsecchi, G., Milani, A., Rossi, A., and Tommei, G., "2004 MN4 Keyholes," *Asteroids, Comets, Meteors*, Cambridge Univ. Press, New York, Aug. 2005.
[27] Chesley, S. R.,"Potential Impact Detection for Near-Earth Asteroids: The Case of 99942 Apophis (2004 MN4)," *Asteroids, Comets, Meteors*, Cambridge Univ. Press, New York, Aug. 2005.
[28] Junkins, J., Singla, P., and Davis, J., "Impact Keyholes and Collision Probability Analysis for Resonant Encounter Asteroids," NASA Workshop on NEO Detection, Characterization, and Threat Mitigation, Vail, CO, NASA White Paper No. 070, June 2006.
[29] Clohessy, W. H., and Wiltshire, R. S., "Terminal Guidance System for Satellite Rendezvous," *Journal of the Aerospace Sciences*, Vol. 27, Sept. 1960, pp. 653–658.
[30] Wie, B.,"Solar Sail Attitude Control and Dynamics: Parts 1 and 2," *Journal of Guidance, Control, and Dynamics*, Vol. 27, No. 4, 2004, pp. 526–544.
doi:10.2514/1.11134
[31] Wie, B., "Thrust Vector Control Analysis and Design for Solar-Sail Spacecraft," *Journal of Spacecraft and Rockets*, Vol. 44, No. 3, 2007, pp. 545–557.
doi:10.2514/1.23084
[32] Wie, B., and Murphy, D., "Solar Sail Attitude Control System Design for a Flight Validation Mission in Sun-Synchronous Orbit," *Journal of Spacecraft and Rockets*, Vol. 44, No. 4, 2007, pp. 809–821.
doi:10.2514/1.22996
[33] Fahnestock, E. G., and Scheeres, D. J., "Dynamical Characterization and Stabilization of Large Gravity Tractor Designs," *Journal of Guidance, Control, and Dynamics* (to be published).
[34] McInnes, C. R., *Solar Sailing: Technology, Dynamics and Mission Applications*, Springer Praxis, New York, 1999.
[35] "Special Edition on Solar Sails," *Journal of Spacecraft and Rockets*, Vol. 44, Nos. 3–4, 2007.
[36] Murphy, D. M., "Validation of a Scalable Solar Sailcraft System," *Journal of Spacecraft and Rockets*, Vol. 44, No. 4, 2007, pp. 797–808.
doi:10.2514/1.23024
[37] Lichodziejewski, D., Derbès, B., Slade, K., and Mann, T., "Vacuum Deployment and Testing of a 4-Quadrant Scalable Inflatable Rigidizable Solar Sail System," 41st AIAA Joint Propulsion Conference and Exhibit, Tucson, AZ, AIAA Paper 2005-3927, July 2005.
[38] Garbe, G., and Montgomery, E., "An Overview of NASA's Solar Sail Propulsion Project," 39th AIAA Joint Propulsion Conference and Exhibit, Huntsville, AL, AIAA Paper 2003-4662, July 2003.
[39] Scheeres, D. J., and Schweickart, R. L., "The Mechanics of Moving Asteroids," 2004 Planetary Defense Conference: Protecting Earth from Asteroids, Garden Grove, CA, AIAA Paper 2004-1440, Feb. 2004.
[40] Izzo, D., Bourdoux, A., Walker, R., and Ongaro, F., "Optimal Trajectories for the Impulsive Deflection of Near-Earth Objects," *Acta Astronautica*, Vol. 59, Nos. 1–5, Apr. 2006, pp. 294–300.
doi:10.1016/j.actaastro.2006.02.002
[41] Izzo, D., "Optimization of Interplanetary Trajectories for Impulsive and Continuous Asteroid Deflection," *Journal of Guidance, Control, and Dynamics*, Vol. 30, No. 2, 2007, pp. 401–408.
doi:10.2514/1.21685